

Influence of manganese doping to the full tensor properties of $0.24\text{Pb}(\text{In}_{1/2}\text{Nb}_{1/2})\text{O}_3\text{-}0.47\text{Pb}(\text{Mg}_{1/3}\text{Nb}_{2/3})\text{O}_3\text{-}0.29\text{PbTiO}_3$ single crystals

Enwei Sun, Rui Zhang, Fengmin Wu, Bin Yang, and Wenwu Cao

Citation: *J. Appl. Phys.* **113**, 074108 (2013); doi: 10.1063/1.4792600

View online: <http://dx.doi.org/10.1063/1.4792600>

View Table of Contents: <http://jap.aip.org/resource/1/JAPIAU/v113/i7>

Published by the [American Institute of Physics](#).

Related Articles

Ferroelectric and dielectric properties of ferrite-ferroelectric ceramic composites

J. Appl. Phys. **113**, 074103 (2013)

Conductivity and frequency dependent specific absorption rate

J. Appl. Phys. **113**, 074902 (2013)

New porous medium Poisson-Nernst-Planck equations for strongly oscillating electric potentials

J. Math. Phys. **54**, 021504 (2013)

Evolution of polar order in $(1-x)\text{Pb}(\text{In}_{1/2}\text{Nb}_{1/2})\text{O}_3\text{-}x\text{PbTiO}_3$ ($0 \leq x \leq 1$) system as investigated by dielectric and Raman spectroscopy

J. Appl. Phys. **113**, 074101 (2013)

Estimation of intrinsic contribution to dielectric response of $\text{Pb}_{0.92}\text{La}_{0.08}\text{Zr}_{0.52}\text{Ti}_{0.48}\text{O}_3$ thin films at low frequencies using high bias fields

Appl. Phys. Lett. **102**, 062906 (2013)

Additional information on *J. Appl. Phys.*

Journal Homepage: <http://jap.aip.org/>

Journal Information: http://jap.aip.org/about/about_the_journal

Top downloads: http://jap.aip.org/features/most_downloaded

Information for Authors: <http://jap.aip.org/authors>

ADVERTISEMENT



AIP Advances

Now Indexed in
Thomson Reuters
Databases

Explore AIP's open access journal:

- Rapid publication
- Article-level metrics
- Post-publication rating and commenting

Influence of manganese doping to the full tensor properties of $0.24\text{Pb}(\text{In}_{1/2}\text{Nb}_{1/2})\text{O}_3\text{-}0.47\text{Pb}(\text{Mg}_{1/3}\text{Nb}_{2/3})\text{O}_3\text{-}0.29\text{PbTiO}_3$ single crystals

Enwei Sun,¹ Rui Zhang,¹ Fengmin Wu,¹ Bin Yang,¹ and Wenwu Cao^{1,2,a)}

¹Condensed Matter Science and Technology Institute, Harbin Institute of Technology, Harbin 150080, China

²Materials Research Institute, The Pennsylvania State University, University Park, Pennsylvania 16802, USA

(Received 18 December 2012; accepted 4 February 2013; published online 21 February 2013)

Complete sets of elastic, piezoelectric, dielectric, and electromechanical properties of $[001]_c$ and $[011]_c$ poled pure and 0.5 wt. % manganese-doped $0.24\text{Pb}(\text{In}_{1/2}\text{Nb}_{1/2})\text{O}_3\text{-}0.47\text{Pb}(\text{Mg}_{1/3}\text{Nb}_{2/3})\text{O}_3\text{-}0.29\text{PbTiO}_3$ single crystals have been characterized at room temperature. The results indicate that manganese ion substitution in the B-site of perovskite $0.24\text{PIN}\text{-}0.47\text{PMN}\text{-}0.29\text{PT}$ single crystals makes the material harder with much higher mechanical quality factor Q_m and slight decrease in piezoelectric and dielectric constants. The much improved Q_m value (200–900) makes Mn-doped single crystals more suitable for high-power transducer applications than pure single crystals. © 2013 American Institute of Physics. [<http://dx.doi.org/10.1063/1.4792600>]

I. INTRODUCTION

Ternary relaxor-based ferroelectric single crystals $x\text{Pb}(\text{In}_{1/2}\text{Nb}_{1/2})\text{O}_3\text{-}(1-x-y)\text{Pb}(\text{Mg}_{1/3}\text{Nb}_{2/3})\text{O}_3\text{-}y\text{PbTiO}_3$ (PIN-PMN-PT) with compositions near the morphotropic phase boundary (MPB) have attracted much attention in recent years for their comparably large piezoelectric and electromechanical properties to that of binary $(1-x)\text{Pb}(\text{Mg}_{1/3}\text{Nb}_{2/3})\text{O}_3\text{-}x\text{PbTiO}_3$ (PMN-PT) single crystals and much higher coercive fields and Curie temperature.^{1–6} Though PIN-PMN-PT single crystals have improved mechanical quality factors ($Q_m \sim 100$) compared to PMN-PT single crystals ($Q_m < 80$), their Q_m are still much too low compared with that of high-power piezoelectric ceramics ($Q_m > 1000$), which significantly hampered their application potential for high-power or resonant-based devices.^{7–9}

Recently, much attention has been focused on the effect of additive on relaxor-PT single crystals, especially manganese (Mn) and iron (Fe) substitutions.^{10–12} It was found that the Fe substitution could enhance the stability of the ferroelectric orthorhombic (FE_O) state of the crystal, resulting larger piezoelectric coefficient, while Mn substitution is effective in inducing hard characteristics, results in larger mechanical quality factor Q_m and coercive field E_c . In order to get a complete picture of the doping effect, the complete matrix of material constants for undoped and Mn-doped ternary relaxor-PT ferroelectric single crystals need to be characterized. More importantly, these complete set of material properties are also essential for the design of electromechanical devices using these crystals.

In this work, we have characterized the complete set of elastic, piezoelectric, and dielectric properties of $[001]_c$ and $[011]_c$ poled pure and 0.5 wt. % Mn-doped $0.24\text{Pb}(\text{In}_{1/2}\text{Nb}_{1/2})\text{O}_3\text{-}0.47\text{Pb}(\text{Mg}_{1/3}\text{Nb}_{2/3})\text{O}_3\text{-}0.29\text{PbTiO}_3$ ($0.24\text{PIN}\text{-}0.47\text{PMN}\text{-}0.29\text{PT}$) ternary single crystals. This composition is only slightly away from the MPB on the rhombohedral phase side, which are selected for their better temperature stability than MPB composition. Four sets of full matrix material properties

were determined using combined resonance and ultrasonic methods because the crystals were poled along $[001]_c$ and $[011]_c$ of the pseudo cubic directions. These self-consistent data sets are much needed for both fundamental understanding of the nature of the ultra-high piezoelectric properties arch as well as input for the design of high-power electromechanical devices using finite element packages. Moreover, the effect of Mn doping on the mechanical quality factor and electromechanical properties of $0.24\text{PIN}\text{-}0.47\text{PMN}\text{-}0.29\text{PT}$ single crystals can be quantitatively revealed.

II. EXPERIMENTAL PROCEDURE

The pure and 0.5 wt. % Mn-doped $0.24\text{PIN}\text{-}0.47\text{PMN}\text{-}0.29\text{PT}$ single crystals used in this work were supplied by H.C. Materials Corp. (Bolingbrook, IL). The crystal boule was grown by the modified Bridgman method and it was found that the content of PIN is insensitive to composition segregation, but the PT content varies along the growth direction.⁵ Samples of desired geometries were cut from the same cross section slice of a crystal boule grown along $[011]_c$ crystallographic direction to maintain the composition uniformity. The dopant amount of Mn was evaluated by the scanning electron microscopy (SEM) with energy-dispersive X-ray spectroscopy (EDS) (FEI Quanta 200) to be ~ 0.5 wt. %.

The as-grown crystals were oriented by the Laue machine with an accuracy of $\pm 0.5^\circ$. Each sample was cut and polished into a parallelepiped with the orientations of $[100]_c \times [010]_c \times [001]_c$ for $[001]_c$ -poled crystals, and $[0\bar{1}1]_c \times [100]_c \times [011]_c$ for $[011]_c$ -poled crystals, respectively. Specimens were annealed at 600°C for 10 h to fill in some of the oxygen vacancies and to reduce residual stress that was developed during crystal growth and mechanical processing. Then, the samples were sputtered with gold electrodes on $[001]_c$ and $[00\bar{1}]_c$, or $[011]_c$ and $[0\bar{1}\bar{1}]_c$ surfaces, and poled at a field of 15 kV/cm for 30 min in silicone oil at room temperature. Each sample was checked for poling completeness using a ZJ-2 piezo d_{33} meter.

The combined resonance and ultrasonic method has proven effective and accurate for getting self-consistent matrix

^{a)}Electronic mail: dzk@psu.edu.

TABLE I. Measured and derived material constants of [001]_c and [011]_c poled pure and Mn-doped 0.24PIN-0.47PMN-0.29PT multidomain single crystals. [Directly measured constants are denoted by star (*).]

		Elastic stiffness constants: c_{ij}^E and c_{ij}^D (10^{10} N/m ²)											
		c_{11}^{E*}	c_{12}^E	c_{13}^E	c_{22}^{E*}	c_{23}^E	c_{33}^E	c_{44}^{E*}	c_{55}^{E*}	c_{66}^{E*}			
Pure	[001]	12.43	10.90	11.02	12.43	11.02	12.45	6.98	6.98	6.21			
	[011]	20.85	12.77	6.07	15.74	12.93	15.39	6.78	0.67	4.87			
Doped	[001]	12.52	10.14	10.33	12.52	10.33	11.74	6.90	6.90	6.41			
	[011]	22.02	13.05	6.46	13.05	10.61	15.85	6.92	0.77	5.87			
		c_{11}^D	c_{12}^D	c_{13}^D	c_{22}^D	c_{23}^D	c_{33}^{D*}	c_{44}^{D*}	c_{55}^{D*}	c_{66}^D			
Pure	[001]	13.51	11.98	8.93	13.51	8.93	16.49	7.49	7.49	6.21			
	[011]	21.27	12.20	7.50	16.51	11.01	20.25	7.27	4.41	4.87			
Doped	[001]	12.81	10.43	9.20	12.81	9.20	16.14	7.37	7.37	6.41			
	[011]	22.11	12.70	7.07	14.43	8.20	20.08	7.30	4.60	5.87			
		Elastic compliance constants: s_{ij}^E and s_{ij}^D (10^{-12} m ² /N)											
		s_{11}^{E*}	s_{12}^E	s_{13}^E	s_{22}^{E*}	s_{23}^E	s_{33}^E	s_{44}^E	s_{55}^E	s_{66}^E			
Pure	[001]	45.76	-19.60	-23.16	45.76	-23.16	49.04	14.33	14.33	16.10			
	[011]	15.65	-24.37	14.59	59.11	-40.13	34.34	14.75	149.25	20.53			
Doped	[001]	32.17	-9.85	-19.64	32.17	-19.64	43.07	14.49	14.49	15.60			
	[011]	15.18	-22.28	8.72	49.49	-24.05	18.85	14.45	129.87	17.04			
		s_{11}^D	s_{12}^D	s_{13}^D	s_{22}^D	s_{23}^D	s_{33}^{D*}	s_{44}^D	s_{55}^D	s_{66}^D			
Pure	[001]	35.84	-29.52	-3.43	35.84	-3.43	9.78	13.35	13.35	16.10			
	[011]	8.20	-6.10	0.51	14.34	-5.62	7.75	13.76	22.68	20.53			
Doped	[001]	24.93	-17.09	-4.47	24.93	-4.47	11.29	13.56	13.56	15.60			
	[011]	9.16	-8.11	0.09	16.21	-3.76	6.48	13.71	21.73	17.04			
		Piezoelectric coefficients: $e_{i\alpha}$ (C/m ²), $d_{i\alpha}$ (10^{-12} C/N), $g_{i\alpha}$ (10^{-3} Vm/N), and $h_{i\alpha}$ (10^8 V/m)											
		e_{15}	e_{24}	e_{31}	e_{32}	e_{33}	d_{15}	d_{24}	d_{31}^*	d_{32}^*	d_{33}^*		
Pure	[001]	8.52	8.52	-9.11	-9.11	17.60	122	122	-646	-646	1285		
	[011]	15.90	7.19	4.98	-6.72	16.88	2373	106	488	-1196	922		
Doped	[001]	6.97	6.97	-4.13	-4.13	16.08	101	101	-408	-408	855		
	[011]	15.08	5.67	2.01	-7.98	13.99	1959	82	330	-776	473		
		g_{15}	g_{24}	g_{31}	g_{32}	g_{33}	h_{15}	h_{24}	h_{31}	h_{32}	h_{33}		
Pure	[001]	7.98	7.98	-15.36	-15.36	30.55	5.97	5.97	-11.86	-11.86	22.92		
	[011]	53.33	9.41	15.26	-37.40	28.84	23.52	6.84	8.46	-11.40	28.63		
Doped	[001]	9.20	9.20	-17.74	-17.74	37.17	6.79	6.79	-7.03	-7.03	27.36		
	[011]	55.20	9.08	18.24	-42.87	26.14	25.40	6.63	4.35	-17.25	30.24		
		Dielectric constants: $\epsilon_{ij}(\epsilon_0)$ and $\beta(10^{-4}/\epsilon_0)$											
		ϵ_{11}^{S*}	ϵ_{22}^{S*}	ϵ_{33}^{S*}	ϵ_{11}^{T*}	ϵ_{22}^{T*}	ϵ_{33}^{T*}	β_{11}^S	β_{22}^S	β_{33}^S	β_{11}^T	β_{22}^T	β_{33}^T
Pure	[001]	1611	1611	868	1728	1728	4753	6.21	6.21	11.52	5.79	5.79	2.10
	[011]	764	1187	666	5028	1273	3613	13.09	8.43	15.02	1.99	7.86	2.77
Doped	[001]	1160	1160	664	1240	1240	2599	8.62	8.62	15.06	8.07	8.07	3.85
	[011]	671	967	523	4010	1020	2046	14.90	10.34	19.13	2.49	9.80	4.89
		Electromechanical coupling factors k_{ij} and density											
		k_{15}	k_{24}	k_{31}^*	k_{32}^*	k_{33}^*	k_t^*	Density (kg/m ³)					
Pure	[001]	0.26	0.26	0.46	0.46	0.89	0.50	8122					
	[011]	0.92	0.26	0.69	0.87	0.88	0.49	8122					
Doped	[001]	0.25	0.25	0.47	0.47	0.86	0.52	8173					
	[011]	0.91	0.23	0.63	0.82	0.81	0.46	8173					

TABLE II. Comparison of piezoelectric constants and mechanical quality factors for pure and Mn-doped 0.24PIN-0.47PMN-0.29PT single crystals.

Samples	Poling directions	Q_{31}	d_{31}	$Q_{31} \cdot d_{31}$	Q_{32}	d_{32}	$Q_{32} \cdot d_{32}$	Q_{33}	d_{33}	$Q_{33} \cdot d_{33}$	Q_t
PIMNT	[001]	94	-646	-60724	94	-646	-60724	35	1285	44975	116
	[011]	156	488	76128	108	-1196	-129168	33	922	30426	104
Mn:PIMNT	[001]	679	-408	-277032	679	-408	-277032	193	855	165015	515
	[011]	432	330	142560	194	-776	-150544	166	473	78518	633

data sets.^{13,14} The dimensions and geometries of samples in resonance measurements were specified by the IEEE standards on piezoelectricity.¹⁵ The resonance and anti-resonance frequencies were obtained by a HP 4194 A impedance-phase gain analyzer. 3 mm cubes with the orientations of $[100]_c \times [010]_c \times [001]_c$ and $[0\bar{1}1]_c \times [100]_c \times [011]_c$ were used for the ultrasonic measurements. A 15 MHz longitudinal wave transducer (Ultran Laboratories, Inc.) and a 20 MHz shear wave transducer (Panametrics Com.) were used for the ultrasonic pulse-echo measurements. The longitudinal transducer was used to measure the phase velocity of longitudinal waves, while the shear wave transducer was used to measure the phase velocity of shear waves. The transducers were excited by a 200 MHz pulser/receiver (Panametrics Com.) and the time of flight between echoes was measured using a Tektronix 460 A digital oscilloscope. The phase velocities of the longitudinal and shear waves were used to calculate the elastic constants together with the density, which was measured by the Archimedes's principle.

III. RESULTS AND DISCUSSION

$[001]_c$ -poled 0.24PIN-0.47PMN-0.29PT single crystal shows tetragonal $4mm$ symmetry macroscopically, which has 11 independent material constants: 6 elastic, 3 piezoelectric, and 2 dielectric constants. But $[011]_c$ -poling induces macroscopic orthorhombic $mm2$ symmetry, which has 17 independent material constants: 9 elastic, 5 piezoelectric, and 3 dielectric constants. We have experimentally determined the complete sets of elastic, piezoelectric, and dielectric constants for both $[001]_c$ and $[011]_c$ poled pure and Mn-doped 0.24PIN-0.47PMN-0.29PT single crystals, and the results are given in Table I. We can see that Mn substitution in PIN-PMN-PT single crystal results in decreased values of piezoelectric constants compared to the pure PIN-PMN-PT. In particular, the d_{33} and k_{33} of $[001]_c$ poled Mn-doped 0.24PIN-0.47PMN-0.29PT single crystal are 855 pC/N and 86%, respectively, which are little lower than that of binary $[001]_c$ poled PMN-28%PT ($d_{33} = 1182$ pC/N, $k_{33} = 91\%$) single crystal, but still much higher than that of Pb(Zr,Ti)O₃ (PZT) ceramics ($d_{33} \sim 400$ pC/N, $k_{33} \sim 70\%$).

The mechanical quality factor Q_m was computed using the relation⁷

$$Q_m = \frac{f_r}{f_1 - f_2}, \quad (1)$$

where f_r is the resonance frequency and f_1 and f_2 are frequencies at 3 dB down the maximum admittances.

Table II compares the piezoelectric constants and mechanical quality factors of pure and Mn-doped 0.24PIN-0.47PMN-0.29PT single crystals under various piezoelectric modes. From Tables I and II, we can see that Mn substitution in PIN-PMN-PT single crystal results in much increased values of mechanical quality factor Q_m , but little decreased values of piezoelectric constants, dielectric constants, and electromechanical coupling factors. These results indicate that Mn substitution in PIN-PMN-PT single crystals induces characteristics of "hard" piezoelectrics.

Fig. 1 shows the temperature dependence of the dielectric constant (ϵ_{33}/ϵ_0) of $[001]_c$ poled pure and Mn-doped 0.24PIN-0.47PMN-0.29PT single crystals at the frequency of 1 kHz. The Mn substitution results in slightly decreased rhombohedral-tetragonal phase transition temperature ($T_{r-t} \sim 109^\circ\text{C}$ for undoping and $T_{r-t} \sim 103^\circ\text{C}$ for Mn-doping) but much increased Curie temperature ($T_c \sim 161^\circ\text{C}$ for undoped and $T_c \sim 192^\circ\text{C}$ for Mn-doping). Fig. 2 shows the polarization hysteresis loops for $[001]_c$ -oriented pure and Mn-doped 0.24PIN-0.47PMN-0.29PT single crystals. The coercive field of Mn-doped crystal ($E_c \sim 8.9$ kV/cm) is much larger than that of pure PIN-PMN-PT crystal ($E_c \sim 5.7$ kV/cm) and the remnant polarization also increased from $26.7 \mu\text{C}/\text{cm}^2$ to $28.2 \mu\text{C}/\text{cm}^2$.

The product $d \cdot Q$ is a very important factor for a piezoelectric resonator because at the resonance frequency, an approximation of the strain x of a longitudinally vibrating bar is given by¹⁶

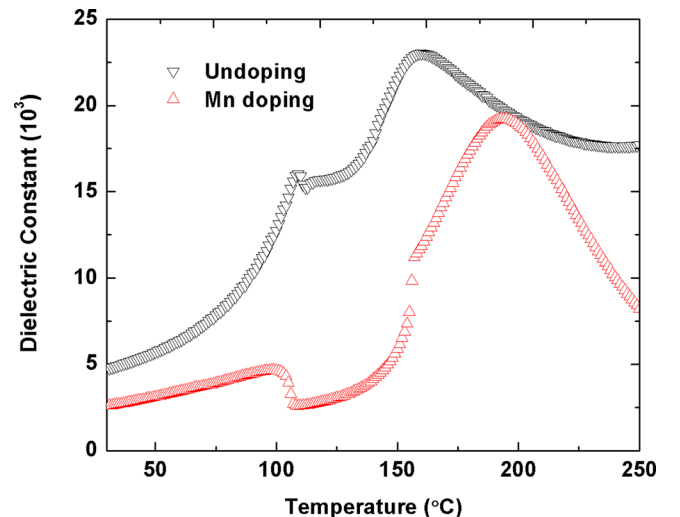


FIG. 1. Temperature dependence of the dielectric constant ϵ_{33}/ϵ_0 for $[001]_c$ poled pure and Mn-doped 0.24PIN-0.47PMN-0.29PT single crystals at the frequency of 1 kHz.

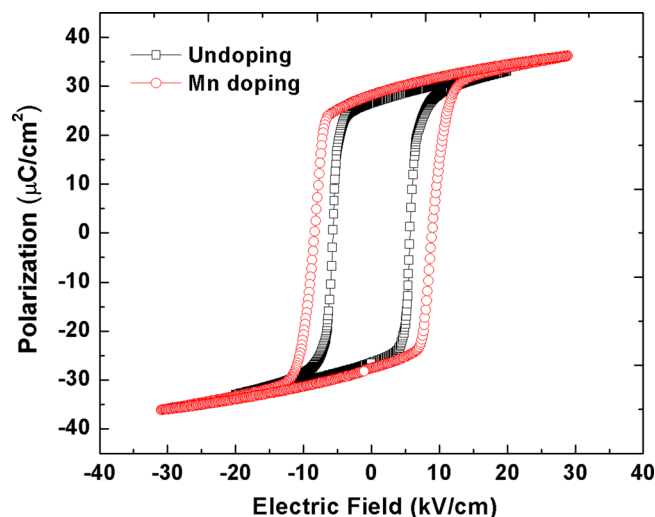


FIG. 2. Polarization hysteresis loops of $[001]_c$ -oriented pure and Mn-doped 0.24PIN-0.47PMN-0.29PT single crystals at room temperature.

$$x = \left(\frac{8}{\pi^2} \right) Q_m d_{31} E, \quad (2)$$

where d_{31} is the transverse piezoelectric constant. This equation shows that an increase of the field induced strain can be obtained by increasing either Q_m or d_{31} . Generally speaking, the higher the Q_m , the narrower is the resonance peak, and accordingly, the higher is the displacement.¹¹ The enhancement in Q_m will lead to reduced self-heating effect,¹⁷ so as to increase the achievable vibration amplitude. The products $d \cdot Q$ for $[001]_c$ and $[011]_c$ poled pure and Mn-doped PIN-PMN-PT single crystals were also listed in Table II. Although piezoelectric constant decreases when Mn-doping modification is introduced, the net result is that the modified crystals have greater $d \cdot Q$ product than undoped crystals. These indicate that the Mn-doped PIN-PMN-PT single crystal has a higher vibration level compared to the pure PIN-PMN-PT single crystal. Therefore, Mn-doped PIN-PMN-PT crystals are more suitable for high-power applications.

As mentioned above, Mn ion can make the 0.24PIN-0.47PMN-0.29PT single crystals to become “harder.” It is known that the “soft” and “hard” characteristics are mainly affected by defects in PZT piezoelectric ceramics. Substituting B sites by lower valence cations (Fe, Mn, Ni, Co) would induce hard piezoelectric behavior.¹⁸ In crystal, doping ions prefer to substitute the ions with equal valence and similar radii according to crystal chemistry principle. It has been demonstrated that Mn acts in the relaxor-PT single crystal as Mn^{2+} by electron spin resonance (ESR) measurements.^{12,18,19} The radius of Mn^{2+} is close to that of Mg^{2+} , Nb^{5+} , or Ti^{4+} , hence Mn^{2+} can be incorporated onto B sites, and oxygen vacancies are created for the charge compensation resulting in defect dipole pairs.^{20,21} The dipole pairs pin the domains, which suppress the dielectric response. In this way, the Mn ion produces “hardening” effects on the 0.24PIN-0.47PMN-0.29PT single crystals.

IV. SUMMARY AND CONCLUSIONS

We have determined the complete sets of elastic, piezoelectric, and dielectric constants for $[001]_c$ and $[011]_c$ poled pure and Mn-doped 0.24PIN-0.47PMN-0.29PT single crystals. These self-consistent complete set of material coefficients are very useful for the design of high-power electromechanical devices as well as for theoretical studies on these relaxor-based domain-engineered single crystals. 0.5 wt. % Mn-doped 0.24PIN-0.47PMN-0.29PT single crystals possess mechanical quality factors as large as 4–5 times of that of undoped PIN-PMN-PT single crystals. Although the piezoelectric coefficient is slightly reduced, the product $d \cdot Q$ is still more than 3 times higher than that of the Mn-doped single crystals compared to the undoped PIN-PMN-PT. Therefore, Mn-doped 0.24PIN-0.47PMN-0.29PT single crystals are much more suitable for high-power electromechanical applications.

ACKNOWLEDGMENTS

This research was supported by the National Key Basic Research Program (973) of China under Grant No. 2013CB632900, the NSFC under Grant Nos. 50602009 and 50972034, and the NIH under Grant No. P41-EB2182. High quality single crystals were provided by H. C. Materials Co., Illinois 60440, USA.

- ¹S. E. Park and T. R. Shrout, *J. Appl. Phys.* **82**, 1804 (1997).
- ²L. C. Lim and K. K. Rajan, *J. Cryst. Growth* **271**, 435 (2004).
- ³Z. Feng, X. Zhao, and H. Luo, *J. Appl. Phys.* **100**, 024104 (2006).
- ⁴Y. Hosono, Y. Yamashita, H. Sakamoto, and N. Ichinose, *Jpn. J. Appl. Phys., Part 1* **42**, 5681 (2003).
- ⁵J. Tian, P. Han, X. Huang, H. Pan, J. F. Carroll III, and D. A. Payne, *Appl. Phys. Lett.* **91**, 222903 (2007).
- ⁶S. Zhang, J. Luo, W. Hackenberger, and T. R. Shrout, *J. Appl. Phys.* **104**, 064106 (2008).
- ⁷S. Priya, K. Uchino, and D. Viehland, *Jpn. J. Appl. Phys., Part 2* **40**, L1044 (2001).
- ⁸S. Zhang, J. Luo, W. Hackenberger, N. P. Sherlock, R. J. Meyer, Jr., and T. R. Shrout, *J. Appl. Phys.* **105**, 104506 (2009).
- ⁹N. P. Sherlock, S. Zhang, J. Luo, H. Y. Lee, T. R. Shrout, and R. J. Meyer, Jr., *J. Appl. Phys.* **107**, 074108 (2010).
- ¹⁰S. Priya, K. Uchino, and D. Viehland, *Appl. Phys. Lett.* **81**, 2430 (2002).
- ¹¹S. Priya and K. Uchino, *J. Appl. Phys.* **91**, 4515 (2002).
- ¹²S. Zhang, L. Lebrun, C. A. Randall, and T. R. Shrout, *J. Cryst. Growth* **267**, 204 (2004).
- ¹³R. Zhang, B. Jiang, and W. Cao, *J. Appl. Phys.* **90**, 3471 (2001).
- ¹⁴E. Sun, S. Zhang, J. Luo, T. R. Shrout, and W. Cao, *Appl. Phys. Lett.* **97**, 032902 (2010).
- ¹⁵ANSI/IEEE Std. 176-1987, *IEEE Standard on Piezoelectricity* (IEEE, New York, 1987), p. 176.
- ¹⁶K. Uchino and S. Hirose, *IEEE Trans. Ultrason. Ferroelectr. Freq. Control* **48**, 307 (2001).
- ¹⁷S. Takahashi, Y. Sasaki, S. Hirose, and K. Uchino, *Mater. Res. Soc. Symp. Proc.* **360**, 305 (1995).
- ¹⁸D. Kobor, L. Lebrun, G. Sébald, and D. Guyomar, *J. Cryst. Growth* **275**, 580 (2005).
- ¹⁹D. Kobor, A. Hajjaji, J. E. Garcia, R. Perez, A. Albareda, L. Lebrun, and D. Guyomar, *J. Mod. Phys.* **1**, 211 (2010).
- ²⁰P. Patnaik, *Handbook of Inorganic Chemicals* (McGraw-Hill, New York, 2001).
- ²¹L. Luo, W. Li, Y. Zhu, and J. Wang, *Solid State Commun.* **149**, 978 (2009).